ELSEVIER

Biophysical Chemistry 92 (2001) 183–199

Biophysical Chemistry

www.elsevier.com/locate/bpc

Molecular dynamics simulation and essential dynamics study of mutated plastocyanin: structural, dynamical and functional effects of a disulfide bridge insertion at the protein surface

Caterina Arcangeli, Anna Rita Bizzarri, Salvatore Cannistraro*

INFM, Dipartimento di Scienze Ambientali, Universitá della Tuscia, Via S. Camillo de Lellis, Blocco D, I-01100 Viterbo, Italy

Received 10 May 2001; received in revised form 17 July 2001; accepted 26 July 2001

Abstract

A molecular dynamics simulation (1.1 ns) at 300 K, of fully hydrated Ile21Cys, Glu25Cys plastocyanin mutant has been performed to investigate the structural, dynamical and functional effects of a disulfide bridge insertion at the surface of the protein. A detailed analysis of the root mean square fluctuations, H-bonding pattern and dynamical cross-correlation map has been performed. An essential dynamics method has also been applied as complementary analysis to identify concerted motions (essential modes), that could be relevant to the electron transfer function. The results have been compared with those previously obtained for wild-type plastocyanin and have revealed that the mutant shows a different pattern of H-bonds, with several interactions lost and a higher flexibility, especially around the electron transfer copper site. The analysis of dynamical cross-correlation map and of essential modes, has shown that the mutant performs different functional concerted motions, which might be related to the binding recognition with its electron transfer partners in comparison with the wild-type protein.

Keywords: Disulphide bond; Poplar plastocyanin; Molecular dynamics; Essential dynamics

* Corresponding author. Tel.: +39-0761-357136; fax: +39-0761-357136.
E-mail address: cannistr@unitus.it (S. Cannistraro).

0301-4622/01/$ - see front matter
PII: S0301-4622(01)00199-5

1. Introduction

Electron transfer (ET) processes play a crucial role in the metabolism of all living organisms, especially in energy converting processes such as photosynthesis and respiration [1,2]. The small blue copper protein plastocyanin (PC) is part of the photosynthetic ET chain [3,4]. The protein is an eight-stranded anti parallel β-barrel macromolecule with a copper atom liganded by the side-chains of two histidine (His37 and His87), a cysteine (Cys84), and a methionine (Met92) in a special geometry described as tetrahedral [5], which is thought to be optimised for ET mediation by means of minimised structural rearrangements upon the redox cycle [6]. Two peculiar surface patches termed hydrophobic and negative patches, are thought to provide the binding interaction sites for the ET physiological partners [4,7].

Among the different experimental approaches, scanning tunnelling microscopy (STM) provides new theoretical progress in studying the ET process of metalloproteins at the level of a single molecule, and might allow one to investigate the ET between a protein molecule and solid state electrodes. Recently, the ET mechanism of azurin (AZ), a blue copper protein whose β-sandwich secondary structure, ET function and spectroscopic features are very similar to those of PC, has been investigated by exploiting its native surface disulphide bridge, which mediates the adsorption onto gold and facilitates the electron tunnel routes [8–10]. On the other hand, early pulse radiolysis experiments performed on wild-type and single-mutated AZ, have shown that an intramolecular ET process from its native reduced disulphide bond to the His46 Cu-ligand occurred, and have suggested a through-bond tunnelling model pathway involving both polypeptide and hydrogen bonds [11]. In order to extend the in situ STM approach to PC, a surface disulfide bridge opposite to the copper site has been introduced by site-directed mutagenesis of both Ile21 and Glu25 replacing them with cysteines [12]. Such an insertion has provided the protein with an anchoring group for gold substrates. The disulfide bridge PC mutant has been demonstrated to be a stable protein and to exhibit spectroscopic features similar to those of wild-type, without significant changes in the copper site structures, even if slight differences in the redox potential and electron paramagnetic resonance (EPR) features between the wild-type and the mutated proteins have been shown [12]. In particular, the larger broadening of the hyperfine pattern observed for the EPR spectrum in the mutated PC compared with the wild-type PC, has been related to an increase in structural heterogeneity of the copper site arrangement [12]. Beside the structural aspects, it should be interesting to investigate whether the introduction of a non-native disulfide linkage into the PC affects the dynamics processes, which are indeed, of main concern for protein functionality. A useful tool for investigating the structural and dynamical behaviour of a protein is represented by the molecular dynamics (MD) simulation, which allows one to extract the temporal and structural fluctuations of both the protein and surrounding solvent at atomic resolution. The MD approach covers the time scale from femto- to nanoseconds, and it is warranted by the fact that the force fields employed are able to reproduce the spectroscopic experiments performed on the same scale. Recently, we have been strongly interested in the application of the MD simulation approach to the study of the dynamical behaviour of both PC and AZ [13–15]. In particular, the deep characterisation of the dynamical behaviour of the wild-type PC by means of MD simulation, has revealed a pronounced stiffness of the hydrophobic and negative patches and of the copper site [13]. Similar results have been found for AZ [14], suggesting that such a peculiar rigidity could be related to the ET mechanism underlying the functionality of these proteins. In addition, the existence of correlated motions between the likely binding sites (i.e. the hydrophobic and negative patches) with the reaction partners and structural regions far from the active site, has suggested that large concerted movements could play an important role for binding recognition between metalloproteins and their physiological ET partners [15].

In the present paper, we present an MD simulation of Ile21Cys, Glu25Cys plastocyanin mutant (PCSS) aimed at investigating the dynamical and

functional effects of the disulfide bond insertion at the surface of the protein. Analysis of concerted motions, which are thought to be relevant for biological function using the essential dynamics (ED) method [16], has also been performed. The comparison of these results with those previously obtained from simulation of wild-type PC [13,15] allow us to show that the dynamics of the protein is affected by mutation. A possible connection between the observed simulated effects and some experimental properties of the PCSS is suggested.

2. Computational methods

PC consists of eight stranded β-strands, arranged in a β-sandwich, connected by random chains (turns) and of a helical insertion (see Fig. 1). The copper site is at the top or Northern end of the protein, surrounded by hydrophobic (12, 33–36, 86 and 89–90 residues) and negative (42–45 and 59–61 residues) patches that are the most relevant surface features of the protein [4,7]. The disulfide bridge has been inserted at the bottom or Southern end of the protein, in order to avoid the perturbation of its active copper site (see Fig. 1).

As the crystal structure of PCSS is not yet available, the initial conformation is represented by the crystal structure of poplar PC solved at 0.133 nm (1PLC entry of Brookhaven Protein Data Bank [17]), where the Ile21 and Glu25 have been replaced with cysteines by means of the SSBOND program [18]. Briefly, the SSBOND program predicts and calculates the conformations with minimal energies for potential disulphide bonds at given sites [18]. The MD trajectories of PCSS have been generated by an integration step of 0.002 ps, using the GROMOS87 program package [19] with the GROMOS force field modified according to Mark et al. [20]. Interaction function parameters for protein atoms have been taken from the standard atom sets in GROMOS87 [19], while appropriate copper–protein interaction parameters have been employed. In particular, because of the strength of the copper interaction with their ligands (His37, Cys84, His87 and Met92), the copper has also been considered to

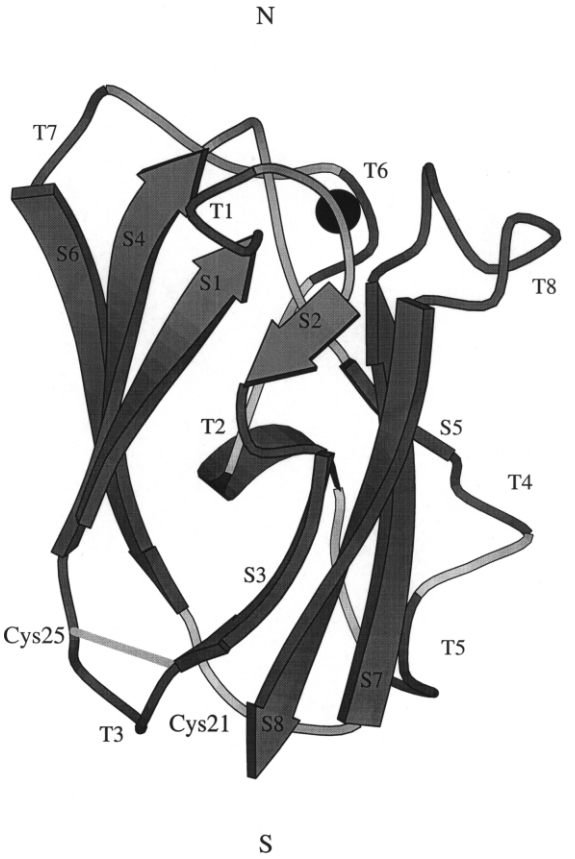

Fig. 1. Model of PCSS structure showing eight β-strands (S1–S8), eight turn regions (T1–T8), and the α-helix. The copper atom (dark sphere) is shown at the top. The mutated residues are labelled and the disulfide bridge is shown. The Northern (N) and Southern (S) end of the protein to which we refer to in the text, are indicated. This drawing was generated using Molscript program [41].

be bound to those residues according to our previous approach [13,14]. This choice, supported on the other hand, by spectroscopic evidence of a covalent nature for the copper-binding site [4], results in a more realistic picture than that obtained with the electrostatic method previously used ([13] and references therein). A similar approach has also been used to treat the PC copper site in a MD simulation work focused on the photo-induced ET dynamics [21]. Here, the coordination bond lengths at equilibria have been derived from the wild-type PC crystal structure

[17] and fixed at $r_0(\mathrm{Cu{-}S_{Cys84}}) = 2.07$ Å, $r_0(\mathrm{Cu{-}N_{His37}}) = 1.91$ Å, $r_0(\mathrm{Cu{-}N_{His87}}) = 2.06$ Å and $r_0(\mathrm{Cu{-}S_{Met92}}) = 2.82$ Å. On the other hand, preliminary crystallographic results on PCSS have indicated that both the copper stereochemistry and the copper–ligand bond lengths are maintained in comparison with the wild-type PC crystal (M. Bolognesi, personal communication). All the ionizable residues, with the exception of copper ligands, have been assumed to be in the ionisation state corresponding to pH 6.0 of the PC crystal. The charge of the copper centre is assumed to be dispersed among the copper ligands and, in analogy to a previous wild-type PC simulation, we have set the charge of Cys84 to -0.5 e, while His37, His87 and Met92 have been considered neutral; a charge of 0.6 e has been assigned to the copper ion. The resulting total protein charge is -7.9 e. The protein molecule has been centred in a truncated octahedron cell filled with 2591 bulk SPC/E waters. To avoid edge effects and to better describe the condition of full hydration, periodic boundary conditions have been applied. Following the same MD simulation protocol adopted for the wild-type PC [13], the cut-off radii of 0.8 nm for non-bonded interactions and of 1.4 nm for long range charged interactions have been used. The system has been minimised to a local minima with the steepest descent method. During the first 105 steps of energy minimisation, a harmonic position restraining a force constant equal to 9000 kJ $\mathrm{mol^{-1}}$ $\mathrm{nm^{-2}}$ has been used to minimise the root mean square deviations from the starting structure. Longer energy minimisation coupled with the conjugate gradient method, have been performed to improve the structure. Initial atomic velocities have been assigned from a Maxwellian distribution corresponding to 250 K. Any residual translational and rotational motion of the centre of mass has been removed from the initial velocities. The temperature has been kept constant at 250 K for the first 6 ps and subsequently, increased by 5 K every 4 ps, to reach a value of 300 K, which has been maintained throughout the following simulation. The temperatures of the protein and of the solvent have been separately coupled to an external bath with relaxation time of 0.5 ps. A decreasing positional restraining force, with a constant going from 9000 to 50 kJ $\mathrm{mol^{-1}}$ $\mathrm{nm^{-2}}$ has been also applied during the first 40 ps. The MD simulation consisted of 100 ps for equilibration followed by 1000 ps of data collection. Configurations of all trajectories and energy have been saved every 0.1 ps and the neighbour pair list has been updated every 10 steps. The Shake constraint algorithm has been used throughout the simulation to fix the internal geometry of water molecules, and to keep bond lengths of protein rigorously fixed at their equilibrium values.

3. Analysis procedures

The dynamical properties of PCSS have been computed by averaging the 100–1100-ps time window. The overall translational and rotational protein diffusions have been removed by superimposing the backbone of each configuration onto the backbone of the starting PCSS structure using a mass-weighted least-squares fitting algorithm [22].

The mass-weighted radius of gyration (R_g) of the PCSS has been calculated according to the equation presented by Arcangeli et al. [14]. The root mean square deviations (RMSD) and fluctuations (RMSF) of atomic positions in the simulation run have been calculated according to:

$$\Delta R = \left[\frac{1}{N_{\mathrm{at}}} \sum_{i=1}^{N_{\mathrm{at}}} \langle \{ (\Delta x_i)^2 + (\Delta y_i)^2 + (\Delta z_i)^2 \} \rangle \right]^{1/2} \quad (1)$$

where N_{at} is the total number of atoms and the brackets $\langle ... \rangle$ represent a time average. In computing the RMSD, Δx_i, Δy_i and Δz_i are the differences between the instantaneous and the starting atomic co-ordinates for the ith atom, while in computing the RMSF, they are the differences between the instantaneous and the averaged atomic co-ordinates for the ith atom.

The frequency of intra protein H-bonds has been computed adopting a geometric criterion to define the formation of a H-bond during the simulation; namely, if the hydrogen to acceptor

distance is shorter than 0.32 nm and the donor–acceptor angle is larger than 120°, a H-bond is assumed to exist [23]. We have considered as maintained the H-bonds, which are present in the simulation with a time percentage greater than 25%; even if the donor or acceptor atom changes during the simulation.

To identify correlated and concerted motions, we have followed two analysis procedures. The first one consists in calculating the dynamical cross-correlation map (DCCM), which is a matrix representation of the time-correlated information between protein atoms i and j, (c_{ij}) [24]:

$$c_{ij} = \frac{\langle r_i r_j \rangle - \langle r_i \rangle \langle r_j \rangle}{\left[\left(\langle r_i^2 \rangle - \langle r_i \rangle^2\right)\left(\langle r_j^2 \rangle - \langle r_j \rangle^2\right)\right]^{1/2}}. \quad (2)$$

The DCCM provides the correlation coefficients for residue displacements along a straight line; positive values are indicative of motions in the same direction, while negative values are indicative of motions in the opposite direction. In order to investigate the convergence speed, we have performed analysis of DCCMs obtained with different averaging time (data not shown). Such an analysis has revealed many differences among the maps, although some elements are maintained in several or all DCCMs, according to what was previously observed for the wild-type PC [13]. Some caution is in order when analysing results corresponding to short averaging time, during which RMSF might not have converged [24]. In addition, the correlation coefficients obtained from the DCCM method do not show any information about the magnitude of the motions; therefore, it may happen that both small- and large-scale collective motions are expressed by the same correlation coefficient [24,25]. To cope with the necessity of separate large-scale correlated fluctuations, which are likely candidates for functionally important motions, using small scale random vibrations, the ED method has also been applied [16,26,27]. Briefly, the method is based on the diagonalisation of the co-variance matrix C_{ij}, built from the atomic fluctuations in a MD trajectory from which overall translational and rotational motions have been removed:

$$C_{ij} = \langle (X_i - X_{i,0})(X_j - X_{j,0}) \rangle \quad (3)$$

where X are the x-, y- and z-co-ordinates of the atoms fluctuating around their average positions X_0. Here, to construct the protein co-variance matrix, the C_α atom trajectory has been used. Indeed, it has been shown that the C_α atoms contain all the information for a reasonable description of the protein large concerted motions [16]. The diagonalisation of the co-variance matrix yields a set of eigenvalues and eigenvectors. The eigenvectors represent a direction in a high-dimensional space, describing concerted fluctuations of atoms. The eigenvalues represent the total mean square fluctuation of the system along the corresponding eigenvectors. By projecting all frames from the MD trajectory on an eigenvector a new trajectory can be generated which, upon visual inspection, reveals the concerted modes, e.g. the modes in which one part of protein tends to act concertedly with another. However, if on one hand, it is assessed that a very small number of essential modes dominate protein motions [16], on the other, these dominant modes change from one sampling window to another and some authors ([15] and references therein, [26]) have reported evidences of insufficient configurational sampling even in nanosecond scale simulations, suggesting that simulations could be unable to provide a reliable eigenvectors set. On the other hand, evidence that a few hundred picoseconds simulation is in general, sufficient to obtain a reasonable convergence of the essential and near constraints subspace is also reported ([15] and references therein). Here, in order to investigate the speed of convergence of the correlated modes, we have analysed the motions along the first three eigenvectors by sampling temporal windows of different lengths of PCSS trajectory (data not shown). Such an analysis has indicated a rapid convergence of fluctuations along the first eigenvectors where relative large and similar concerted motions are found after 200 ps (data not shown).

Table 1
Selected properties of PCSS calculated from the MD simulated trajectories[a]

Parameter	Mean	S.D.[b]	Min.[c]	Max.[d]	Drift[i]
R_g (nm)[f]	1.233	0.006	1.211	1.241	0.008
E_{pot} (MJ/mol)[g]	−159.27	0.51	−157.78	−161.80	−0.33
E_{kin} (MJ/mol)[h]	29.85	0.24	28.96	30.91	0.03
All atom RMSD[e] (nm)	0.184	0.021	0.126	0.248	0.050
C_α atom RMSD (nm)	0.151	0.021	0.087	0.219	0.050

[a]All values are calculated during the 100–1100-ps time interval.
[b]S.D.: standard deviation.
[c]Min: minimal value.
[d]Max: maximal value.
[e]RMSD: root mean square deviations.
[f]R_g: radius of gyration.
[g]E_{pot}: total potential energy.
[h]E_{kin}: total kinetic energy.
[i]The drift values are calculated from a linear regression and are given per picosecond.

Examinations of the molecular structures and analyses of the trajectories have been carried out using the WHAT-IF modelling program [28] and the ED routines supplied therein.

4. Results

4.1. Stability of the simulation

The stability of the simulation has been checked by computing a set of geometrical and energetic properties. The time-averaged values of the R_g, of the total potential and kinetic energies and of the RMSDs from the initial protein structure are reported in Table 1. The parameter R_g, a property linked to the protein volume, fluctuates around a mean value of 1.233 nm, which is very close to that found for the wild-type PC (1.235 nm). The mean values of the total potential and kinetic energies are comparable with those observed for wild-type PC [13], and their time evolution reveals that after approximately 48 ps, both types of energies are almost unchanged and practically stable after 100 ps (data not shown). The overall RMSDs, calculated with respect to the initial structure, which are found to be slightly higher (0.184 and 0.151 nm for all atoms and C_α atoms, respectively) than those found for wild-type PC (0. 174 and 0.141 nm for all atoms and C_α atoms, respectively), indicate a small displacement from the initial structure during all of the simulation run. The RMSDs of PCSS from the initial structure, which is a function of simulation time, are plotted in Fig. 2. For comparison, the RMSDs of wild-type PC (broken line) are also shown in the same figure. In both of the simulated structures, an initial rise is followed by small fluctuations between 0.15 and 0.22 nm. Although the RMSD for the PCSS structure appears to rise slightly even after 800-ps simulation, the drift value obtained is quite low and comparable to those obtained for other protein simulations [24], indicating that both protein structures are practically stable after 100 ps. In the inset of Fig. 2, the time evolution of the radius of gyration of PCSS is reported. The PCSS gyration radius reveals an initial rapid increase (which is consistent with the solvation of charged and polar residues on the protein surface), a slow decrease after 150 ps, and a fluctuation around a stable value after 470 ps. The overall picture is that, similarly to wild-type PC, the mutant maintains its globular shape and is almost stable during all of the simulation run.

4.2. Structure and dynamics of the mutant: a comparison with the wild-type protein

The comparison between the time-averaged (over 1000-ps simulation) simulated structure of

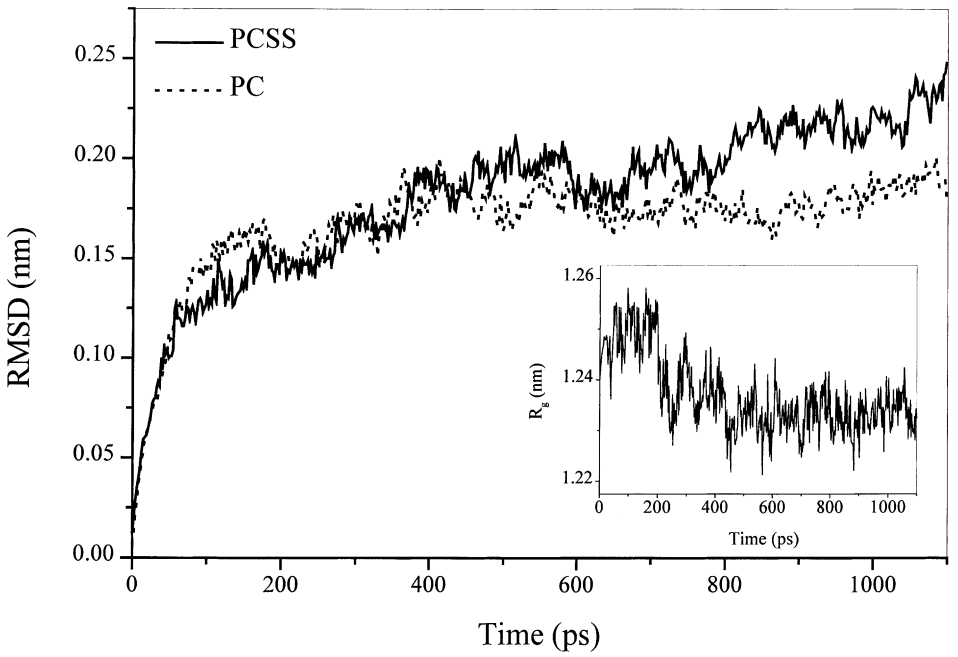

Fig. 2. The root mean square deviations (RMSDs) of all atoms of PCSS (solid line) and wild-type PC (broken line) as a function of simulation time. Inset: the radius of gyration of PCSS as a function of simulation time.

the mutant and of the wild-type PC is shown in Fig. 3A, where the C_α atom trace of the mutant (light grey) superimposed on those of wild-type PC (dark grey) is depicted. The two overall protein structures are remarkably similar, although some differences can be observed in specific regions, i.e. the T8 turn, which is close to the ET copper centre and contains two copper ligands (His87 and Met92). As already mentioned, the copper site represents the protein functional group and its peculiar co-ordination geometry is characteristic of all the blue copper proteins. Such a peculiar copper site geometry confers to metalloproteins their typical spectral properties of an intense blue colour, a narrow hyperfine splitting in the EPR spectrum, and a strong resonance Raman peak at approximately 400 cm^{-1} [29–31]. From an evolutionary viewpoint, such a tetrahedrally distorted geometry is the most appropriate because the blue copper proteins are ET proteins and small changes in geometry give rise to small reorganisational energy and thus, a high rate of ET [1,6]. To focus on the structural effects occurring to the functional copper site, a comparison between the PCSS (light grey) and wild-type (dark grey) copper sites is depicted in Fig. 3B. In this respect, one should take into account that even if the bonded approach used to treat the copper site could restrain the copper ligand distances, some rearrangements of the active site might be possible. Fig. 3B shows that the copper centres are very similar and display the same co-ordination geometry. Indeed, the time-averaged atomic positions of the sulfur (S) and nitrogen (N) atoms liganded to the copper are maintained both protein structures. Only small differences concerning the atomic positions of the Met92 and His87 atomic chains between the mutant and wild-type structures are observed. Therefore, the introduction of the disulfide bridge at the protein surface has only modest effects on the structure and geometry of the ET copper site. Such findings agree with experimental investigations, which have demonstrated that the mutant displays absorption and Raman spectra very similar to those of wild-type PC [12], and with preliminary crystallo-

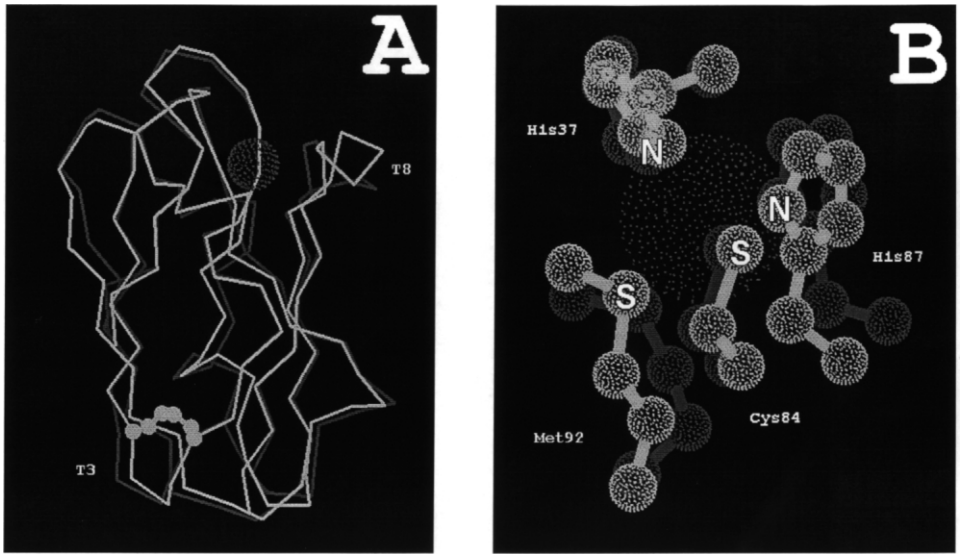

Fig. 3. (A) Superposition of the C_α atoms of PCSS (light grey) onto those of wild-type PC (dark grey). The copper atom (dark sphere) and the disulfide bridge (ball and stick) are also shown. (B) Picture of the superposition between PCSS and wild-type PC copper ligands (ball and stick). The sulfur (S) and nitrogen (N) atoms liganded to the copper are also labelled. The drawings were generated using the WHAT-IF modelling program [28].

graphic results, which have shown that both copper stereochemistry and copper-ligand bond lengths are maintained in the mutant crystal (M. Bolognesi, personal communication).

To gain a deeper insight into the structural rearrangements occurring in the mutant, the PCSS intrinsic H-bonding network, which is strictly related to the maintenance and stabilisation of the secondary structure elements, has been investigated. Fig. 4 shows a diagram of the secondary structure elements, the H-bonds present in the simulated PCSS structure, the hydrophobic and negative patches, the disulphide bridge and the copper ion. The H-bond network involving backbone atoms is particularly important to maintain and stabilise the secondary structure elements. Indeed, a comparison with the wild-type PC data [13] reveals a close similarity, which is particularly evident in the two β-sheets forming the PC scaffold. Such a finding suggests that the introduction of the disulfide bridge does not affect the secondary structure of the mutant. However, the mutation appears to cause the loss and formation of H-bond interactions in correspondence with some functional negative and hydrophobic residues. A new H-bond interaction between the negative Ser45 and the Ser81 is registered in the PCSS structure. Of particular interest are the rearrangements occurring in the T8 turn, which actually belongs to one of the most crucial regions of the protein, since it contains two copper ligands (His87 and Met92) and most of the hydrophobic residues, that are involved in the ET mechanism [4,7]. In particular, three H-bonds present in the wild-type structure and connecting the T8 turn to S7 and S8 β-strands are lost and replaced in PCSS by four new ones occurring within the T8 turn (His87–Met92, His87–Gly91, His87–Ala90, and Gln88–Gly91). Moreover, two H-bond interactions (Gly91–Phe14 and Ser85–Asn38), present in the wild-type PC structure, are definitively lost in PCSS, possibly conferring a higher mobility to the T8 turn. Concerning the side-chain H-bond pattern, even if some interactions (namely the Phe41–Ser56, Asn64–Glu68 and Ala65–Glu68 H-bonds), which are important to stabilise loops and β-strands are conserved, several others are definitively lost in PCSS.

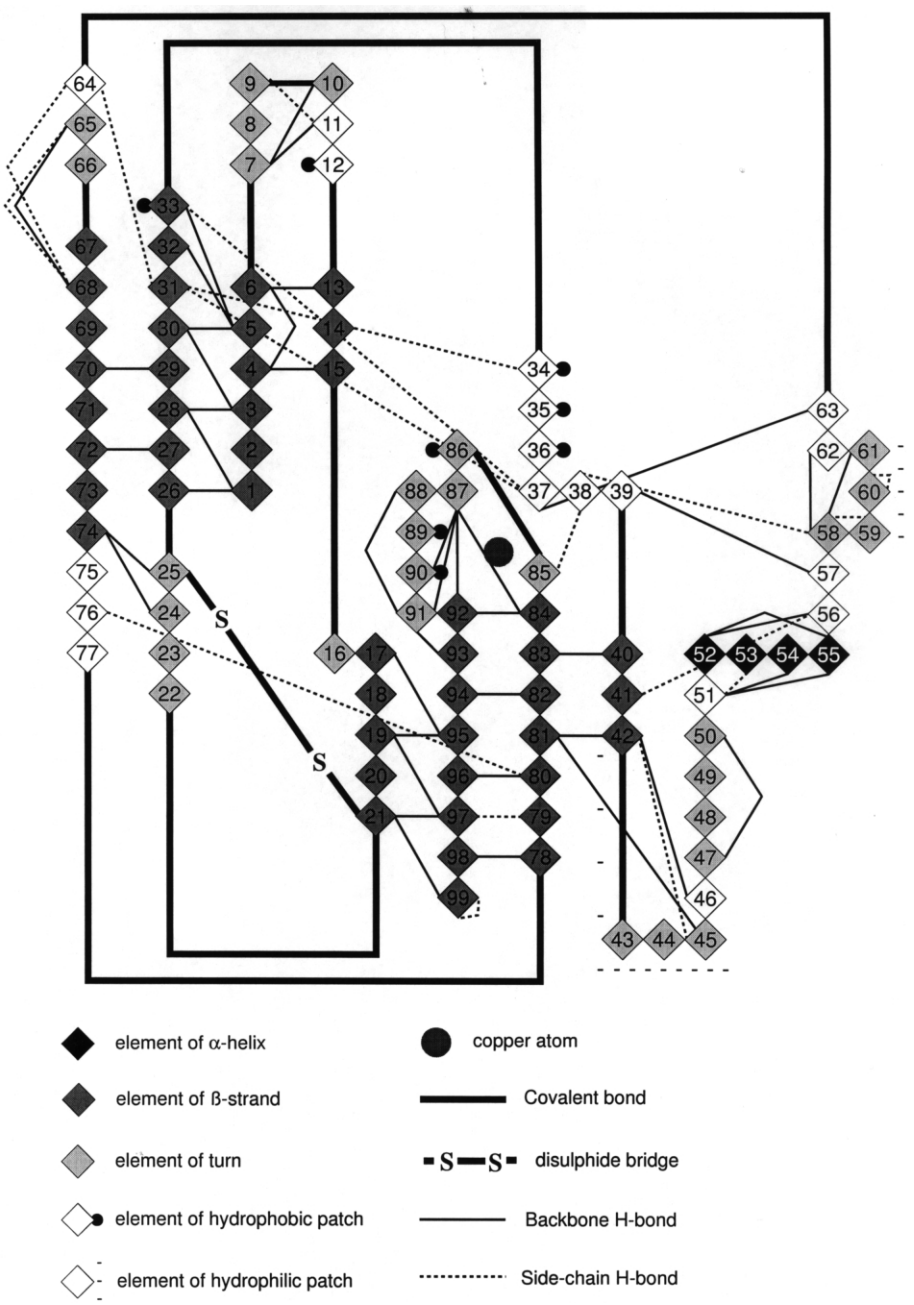

Fig. 4. Diagram of secondary structure elements of PCSS with the simulated H-bonding pattern. Grey intensity represents the secondary structure of amino acids. The copper atom, the disulphide bridge, and the hydrophobic and negative patches are also indicated.

Besides a stabilisation of the secondary and tertiary structure of the molecule, the side-chain H-bond interactions may play an important role for the functionality of the protein. In this re-

spect, a recent hypothesis concerning the involvement of hydrogen bonds in the ET mechanism has been put forwarded [32]. Indeed, there is considerable experimental evidence for ET over long distances through saturated bonds whose electronic interactions decrease exponentially with distance [32]. In this respect, the side-chain H-bonds, which are important for the geometry of the copper site as well as for the connection of the Cu-site to a probable ET pathway, are maintained in the PCSS structure. In particular, the Ala33–His37 H-bond that occurs in both the PCSS and wild-type structures, is a crucial interaction in stabilising the orientation of the imidazole ring of His37, one of the Cu-ligand residues [17]. The Asn38–Ser85 H-bond is involved both in the interaction, which establish the copper site geometry, and in the relationship between the copper site and the part of the putative electrostatic recognition path [17]. Indeed, the residue 85 is adjacent to the Cys84, the Cu-ligand residue which is almost certainly part of an ET pathway to and from the copper site. It is known that the negative patch to which Glu59 belongs, surrounding the nearly conserved residue Tyr83, is implicated in one of the two ET pathways [4] and in this respect, we note that the Glu59–Tyr83 H-bond, present in the crystal structure of wild-type PC, is lost in PCSS. In the mutated PC, one could suppose that an alternative ET path via the Ser58–Asn38 and Asn38–Ser85 H-bonds, and through the Ser85–Cys84–Tyr83 covalent bonds might occur. In addition, the Asn76–Tyr80 interaction, present in both the PCSS and PC structures, appears to play a role in the formation of the so-called tyrosinate, which is supposedly responsible for the peculiar red-shifted fluorescence emission [33].

The backbone RMSFs, which describe the flexibility about the mean structure, have been used to determine the mobility along the sequence and to enlighten differences in the dynamical behaviour of the mutant. The PCSS relative mobility has been calculated from the time-averaged (over 1000-ps simulation) backbone RMSFs and depicted in Fig. 5a, where the structure elements are coloured according to relative motion from light grey (low mobility) to dark grey (high mobility). For comparison, the wild-type PC relative mobility is also shown in Fig. 5b. Both the simulated structures display highest mobility (dark grey) in correspondence of the surface regions, especially in turn regions; low values of fluctuation (light grey) are, on the contrary, observed for residues forming the β-strands. However, we note that the PCSS fluctuations are, on the average, higher (0.097 nm) than those registered for wild-type PC (0.070). The mutation has only modest effects on the mobility of T3 turn, indicating that the insertion of the disulphide bridge does not affect the fluctuations in this region. However, significant differences have been found in correspondence with the T7 and T8 turns, which show much higher mobility in PCSS (see Fig. 5a) than in wild-type PC (see Fig. 5b). This flexibility seems to be also reflected in the peculiar H-bond pattern in correspondence to the T8 turn, where a number of interactions are lost (see Fig. 4). As already mentioned, the T8 turn contains a number of hydrophobic residues which are believed to be crucial for the ET function [4,7] and the His87 and Met92 copper ligands. On the other hand, the pronounced stiffness observed in both the wild-type PC [13] (see Fig. 5b) and AZ has been correlated to the ET process exerted by these proteins [14]. It is believed that molecular vibrations assist the ET process and that small rearrangements of protein residues proximal to the peculiar tetrahedral distorted copper reaction centre, modulate the value of the redox potential and optimise the fine tuning of the ET reaction [6,34]. The high mobility in residues near the copper ET site of the mutant could be related to dynamical differences in performing the ET function. In addition, the higher copper site flexibility appears to be in agreement with the enhanced structural heterogeneity in the copper site geometry, as revealed by EPR data found for the mutant [12]. Actually, since the intrinsic topological disorder is connected to the existence of a huge amount of conformational sub-states explored by the protein during its dynamical evolution [35], the high values of fluctuations registered for the residues near the copper site, could reflect a higher conformational variability for the mutant in comparison with the wild-type PC. Therefore,

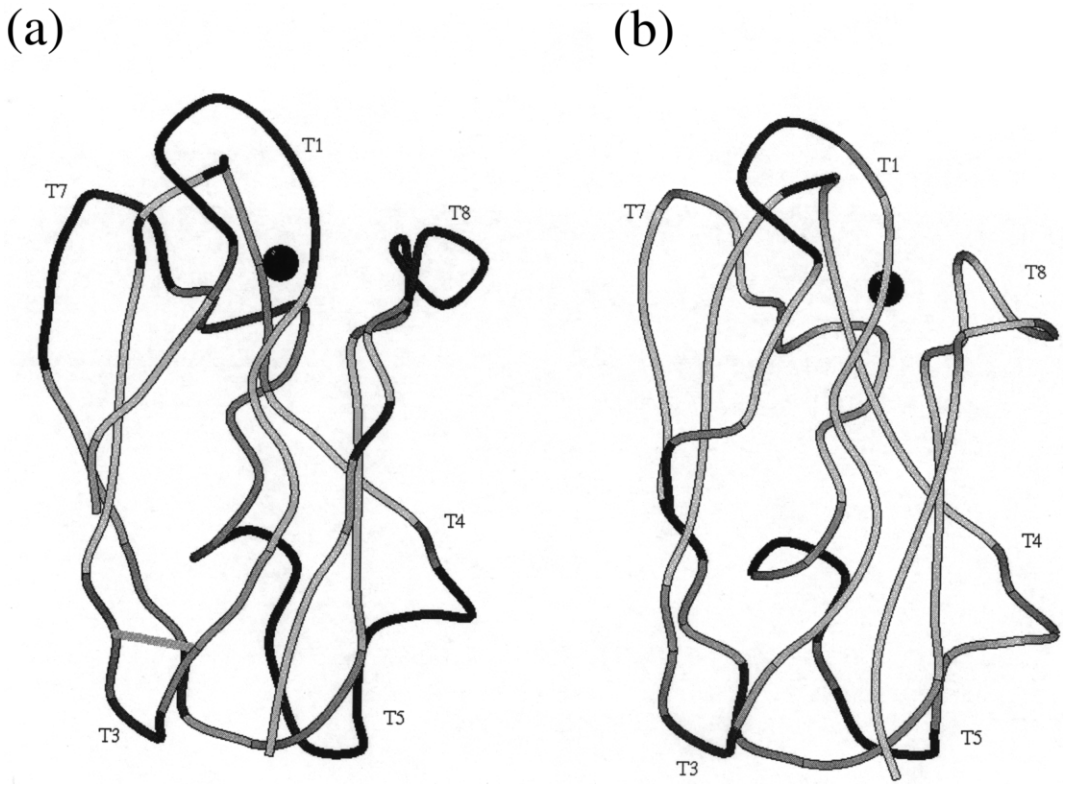

Fig. 5. Main-chain C_α traces of PCSS (a) and wild-type PC (b) depicting relative mobility as determined from the time-averaged backbone RMSFs. Structure elements are coloured according to the relative motion from light grey (low mobility) to dark grey (high mobility).

the mutant could explore a higher number of configurational sub-states corresponding to structural arrangements of some group of atoms.

4.3. Correlated and concerted functional motions

The knowledge of the collective character of motions in proteins is crucial for the understanding of their biological function [36]. Actually, relative and concerted movements between groups of protein atoms (small domains) could determine large-scale conformational transitions, providing a wide range of protein conformations with small expenditure in energy. Each small domain would represent a structurally rigid entity composed of amino acids residues that move both co-operatively and coherently. In the ET copper-proteins, concerted motions between the binding sites and other different protein domains could be crucial for the partner recognition. Indeed, a previous investigation performed on wild-type PC and AZ has evidenced the existence of concerted motions among the binding sites and structural regions far from the copper site [15]. In addition, simulation studies have shown that the binding and protein docking between PC and its physiological partners are dynamical mechanisms and configurational fluctuations and structural rearrangements in the proteins underlie such processes [37,38].

To look into the functional motions, we have analysed the collective character exhibited by the mutated protein by means of DCCM and the ED method. The DCCM, which reports the time-correlated motions of atomic pairs, obtained for PCSS is shown in Fig. 6. We observe that a number of clusters are present in the upper left

triangle. Several of them, located around position (3, 15), (4, 30), (29, 69), (18, 95), (80, 95), (41, 82) and (18, 80), represent positively correlated motions between pairs of adjacent β-strands. With the exception of the last, the same clusters are also present in the DCCM of wild-type PC [13]. The characteristic diagonal shape, with an ascending or descending trend, is respectively correlated to the parallel or anti parallel coupling of strands in the tertiary structure. In comparison with wild-type PC results [13] a number of new positive clusters, indicating correlated motions among functional residues (represented by open squares), occur in PCSS.

In particular, the (5, 89) and (24, 88) clusters represent the correlated motions among the S1 β-strand and the T3 turn with the T8 turn. It should be noted that within the T3 turn is located the disulfide bridge insertion while the T8 turn contains the 86, and 89–90 hydrophobic residues as well as the His87 and Met92 copper-ligands. In addition, we remark that such clusters are indicative of correlated motions among protein regions that are far apart in the tertiary structure. We observe also a positively correlated cluster around (34, 48) residues, which lie close in the folded protein; it represents concerted motions between functional 'domains' involving negative and hydrophobic residues surrounding the copper ion. The (8, 47) cluster correlates positively the motion of the hydrophobic Leu12 with that of the negative Asp42 residue. It is interesting to note that the Leu12 residue, that is a highly conserved residue, has been found to be crucial for binding

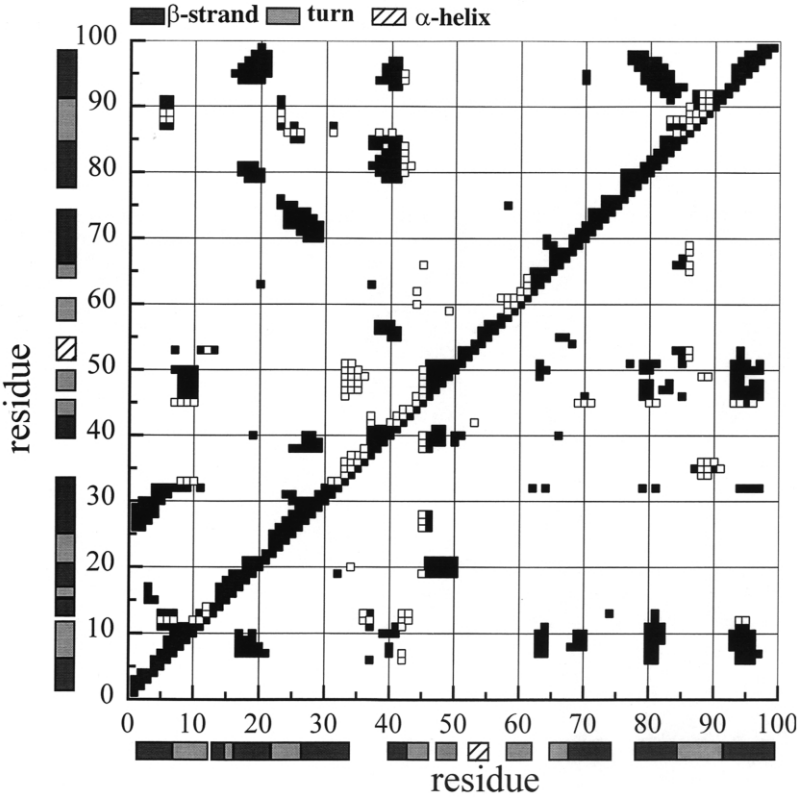

Fig. 6. Dynamical cross-correlation map (DCCM) for the C_α atom pairs of PCSS averaged over a 100–1100-ps time interval. Only correlation coefficients with an absolute threshold value greater than 0.3 are shown. Positive correlations (motions in the same direction) are mapped in the upper left triangle, and negative correlations (motions in opposite direction) in the lower right triangle. Open squares: functional hydrophobic and negative residues. Secondary structure elements are also shown.

recognition with the physiological reaction partner [4,39]. Of particular interest are the negative interactions shown in the lower right triangle of DCCM. Negative correlations occur mostly among residues that are far apart in the tertiary structure of the protein, even if some clusters involve residues, which are close in space. With the exception of clusters located around (19, 6), (63, 6), (69, 6) and (81, 6), which represent anti-correlated motions between the T1 turn with the S3, S6, S7 and S8 β-strands, most of the negative clusters are indicative of anti-correlated motions between those regions, which are putatively implied in the ET process. In particular, the clusters around (47, 38), (47, 20) and (47, 29) residues represent anti-correlated motions among the negative Ser45 residue with S4 and S5 β-strand and the T3 turn. The clusters located around (87, 35), (86, 52) and (86, 65) are indicative of anti-correlated motions of the T8 turn, which represent that region of protein mostly rich in hydrophobic residues and Cu-ligands, with protein regions which are far apart in the tertiary structure. Such a behaviour suggests that small protein regions, remote from the copper site, move in a concerted way with far protein portions, which are close to the copper reaction centre. In this respect, experimental and simulated studies on the PC system suggested that the specific protein motions coupled to the ET, also involve directional correlated motions of atoms far from the copper site [31,21].

The overall emerging picture is that, similarly to wild-type PC [13], all the secondary structural elements within the PCSS move in an approximately concerted fashion and that correlated motions among turn regions, which are putatively implied in the ET process occur. However, it should be remarked that in DCCM analysis when two atoms move exactly in phase and with the same period, but along perpendicular lines, will have a correlation coefficient value of zero, which means that a number of motions are counted as totally uncorrelated [24,25]. In addition, the correlation coefficients obtained from the DCCM method do not bear any information about the magnitude of the motions; therefore, it may happen that both small- and large-scale collective motions were expressed by the same correlation coefficient [24,25]. In order to separate large-scale correlated fluctuations, likely candidates for functionally important motions, from small-scale random vibrations, we have further analysed the MD trajectories of PCSS according to the ED approach.

In such an approach, the most important motions of the protein are extracted from the trajectory by principal component analysis of the Cartesian co-ordinate covariance matrix, yielding eigenvectors and corresponding eigenvalues (see analysis procedures). The eigenvectors with the largest associated eigenvalues define the essential subspace in which most of the protein dynamics occurs.

The present ED results indicate that a few eigenvectors suffice to describe the dynamics of the mutant and that approximately 80% of the total protein motion is described by the first 30 eigenvectors (data not shown). Such results are closely similar to those found for the wild-type PC [15]. In agreement with the wild-type PC results [15], motions along the first four eigenvectors describe non-Gaussian, i.e. non-harmonic, fluctuations (data not shown).

The onset of anharmonic motions is believed to be important in order to activate the transition among the conformational sub-states, whose sampling is relevant for biological functionality [35]. Here, we have investigated the motions along such non-Gaussian eigenvectors by projecting all the trajectory frames onto the specific eigenvector; the newly generated trajectory reveals a motion in the direction defined by the eigenvector [16,40]. A pictorial view of the PCSS motions along the first three eigenvectors of C_α co-variance matrix is shown in Fig. 7a. To emphasise the differences with respect to the wild-type protein, the authors have also shown the essential motions along the first three eigenvectors of wild-type PC (Fig. 7b) obtained from a previous simulation and ED analysis [15]. By comparing the PCSS and the wild-type PC motions it appears that the introduction of the disulphide bridge at the surface T3 turn deeply modifies the concerted behaviour of the mutant, especially along the first two eigenvectors. Indeed, the motion along the first PCSS eigenvector shows that the surrounding copper

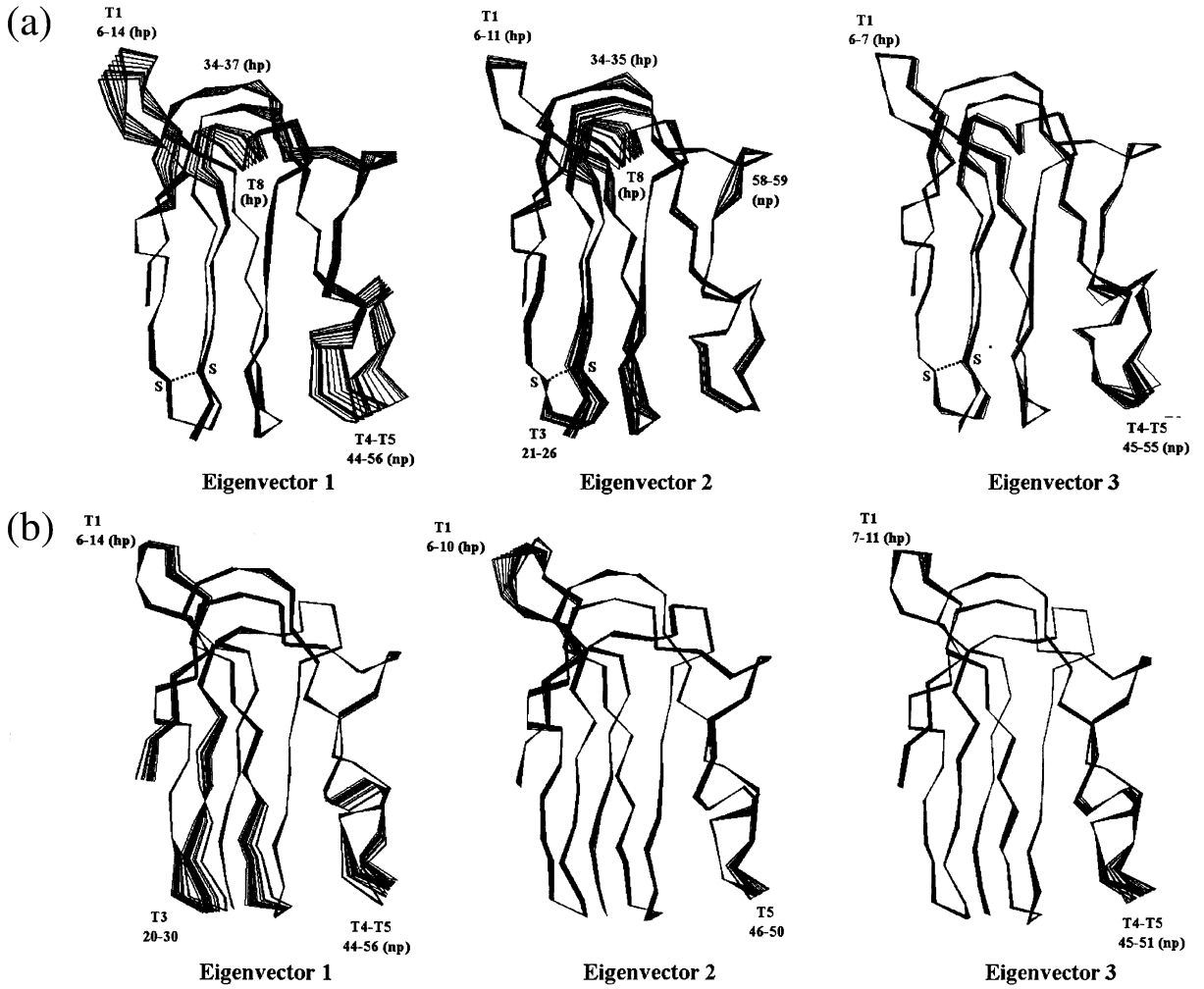

Fig. 7. Twenty-five frames taken at equally spaced intervals from the motions along the first three eigenvectors of the PCSS (a) and wild-type PC (b) co-variance matrices constructed over 1000-ps simulations. The structural regions, residue numbers, negative (np) and hydrophobic (hp) patches are also indicated. The drawings were generated using the WHAT-IF modelling program [28].

residues (the hydrophobic 6–14, 34–37 and 86–92 residues) move concertedly with the remote negative (43–45 residues) patch. The mutated region (T3 turn) does not appear to be involved in such motions. A different situation is observed along the first wild-type PC eigenvector; the hydrophobic turn (6–14 residues) close to the copper site moves concertedly with regions far away from the active site, namely the negative 46–56 residues, the T3 turn and the S6 β-strand. The motion along the second PCSS eigenvector concerns the motions of the T7 turn and both the hydrophobic (6–11, 34–35, and 85–92 residues) and negative (58–59 residues) patches, close to the active site, with the disulphide bridge (T3 turn) and the S6 β-strand which are far away from the copper ET site. The motion along the second wild-type PC eigenvector shows that only the T1 turn, located at the top of the protein, moves in a concerted fashion with the remote negative 47–52 patch. Finally, the motion along the third PCSS eigenvector concerns the

concerted motions of the functional T5 turn, containing the 45–55 residues which are located in the negative patch, and the T3 and T7 turns which are opposite to the copper site. A similar behaviour is observed for the wild-type PC motion along the third eigenvector. By resuming, it appears that the ED method has proved to be an appropriate method for enlightening the differences about the functional concerted motions performed by the mutant. Such differences, which are particularly evident along the first two eigenvectors describing non-harmonic fluctuations, could reflect a different way in which the mutated protein performs the functional fluctuations related to the binding recognition with its ET partners.

5. Conclusions

MD simulation has proved to be a useful tool to investigate the structural, dynamical and functional effects of the introduction of a non-native disulfide bridge at the plastocyanin surface.

The analysis of the simulation stability has revealed that the mutant maintains its globular shape and is almost stable during all the simulation run. A detailed analysis of the simulated H-bond pattern has evidenced that the introduction of the disulphide bond at the protein surface does not affect the secondary structure as well as the peculiar co-ordination copper geometry of the protein. Such results are in agreement with the experimental spectroscopic data that have indicated mutant spectroscopic features similar to those of wild-type PC [12]. Analysis of the RMSFs, describing the protein flexibility, has revealed that the introduction of the disulfide bridge at the surface of the protein, affects the dynamical fluctuations around the copper ET site. The higher mobility within residues near the copper reaction centre seems to be in agreement with the enhanced structural heterogeneity found for the mutant suggesting an higher conformational variability [12]. Analysis of DCCM has indicated the presence of correlated motions among protein regions, which are supposed to be involved in the ET mechanism. The results are very similar to those obtained for the wild-type PC [13]. On the other hand, the ED method has been proved to be appropriate to separate small- from large-scale motions, which are likely candidates for functionally important motions. Indeed, the analysis of the essential modes describing non-harmonic fluctuations has enlightened a different way in which the mutated protein performs the functional fluctuations related to the binding recognition with its ET partners.

Acknowledgements

The present work has been partly supported by a PRIN-MURST project. Thanks are due to Prof. Martino Bolognesi (University of Genova, Italy) for communication about the preliminary crystallographic results.

References

[1] R.A. Marcus, N. Sutin, Electron transfer in chemistry and biology, Biochim. Biophys. Acta 811 (1985) 268–322.
[2] R.J.P. Williams, Electron transfer in biology, Mol. Phys. 68 (1989) 1–23.
[3] E.T. Adman, Topics in molecular and structural biology: metalloproteins in: P.M. Harrison (Ed.), Structure and Function of Small Blue Copper Proteins, vol. 6, part I, Chemie Verlag, Weinheim, 1985, pp. 1–42.
[4] M.R. Redinbo, T.O. Yeates, S. Merchant, Plastocyanin: structural and functional analysis, J. Bioenerg. Biomembr. 26 (1994) 49–66.
[5] M. Guss, H.C. Freeman, Structure of oxidized poplar plastocyanin at 1.6-Å resolution, J. Mol. Biol. 169 (1983) 521–563.
[6] W.E.B. Shepard, B.F. Anderson, D.A. Lewandoski, G.E. Norris, E.N. Baker, Copper co-ordination geometry in azurin undergoes minimal change on reduction of copper(II) to copper(I), J. Am. Chem. Soc. 112 (1990) 7817–7819.
[7] O. Farver, Y. Shahak, I. Pecht, Electron uptake and delivery sites on plastocyanin in its reaction with the photosynthetic electron transport system, Biochemistry 21 (1982) 1885–1890.
[8] E.P. Friis, J.E.T. Anderson, L.L. Madsen, P. Møller, J. Ulstrup, In situ STM and AFM of the copper protein *Pseudomonas aeruginosa* azurin, J. Electroanal. Chem. 431 (1997) 35–38.

[9] E.P. Friis, J.E.T. Anderson, Y.I. Kharkats et al., An approach to long-range electron transfer mechanisms in metalloproteins: in situ scanning tunneling microscopy with submolecular resolution, Proc. Natl. Acad. Sci. USA 96 (1999) 1379–1384.

[10] J.J. Davis, C.M. Halliwell, H.A.O. Hill, G.W. Canters, M.C. van Amsterdam, M.Ph. Verbeet, Protein adsorption at a gold electrode studied by in situ scanning tunnelling microscopy, New J. Chem. 22 (1998) 1119–1123.

[11] O. Farver, L.K. Skov, G. Gilardi et al., Structure–function correlation of intramolecular electron transfer in wild-type and single-mutated azurins, Chem. Phys. 204 (1996) 271–277.

[12] L. Andolfi, S. Cannistraro, G.W. Canters, P. Facci, A.G. Ficca, I.M.C. Van Amsterdam, M.Ph. Verbeet, A poplar plastocyanin mutant suitable for adsorption onto gold surface via disulphide bridge, Biochemistry (2001) (submitted).

[13] A. Ciocchetti, A.R. Bizzarri, S. Cannistraro, Long-term molecular dynamics simulation of copper plastocyanin in water, Biophys. Chem. 69 (1997) 185–198.

[14] C. Arcangeli, A.R. Bizzarri, S. Cannistraro, Long-term molecular dynamics simulation of copper azurin: structure, dynamics and functionality, Biophys. Chem. 78 (1999) 247–257.

[15] C. Arcangeli, A.R. Bizzarri, S. Cannistraro, Concerted motions in copper plastocyanin and azurin: an essential dynamics study, Biophys. Chem. 90 (2001) 45–56.

[16] A. Amadei, A.B.M. Linssen, H.J.C. Berendsen, Essential dynamics of proteins, Proteins: Struct. Funct. Genet. 17 (1993) 412–425.

[17] J.M. Guss, H.D. Bartunik, H.C. Freeman, Accuracy and precision in protein structure analysis: restrained least-squares refinement of the structure of poplar plastocyanin at 1.33-Å resolution, Acta Cryst. B48 (1992) 790–811.

[18] B. Hazes, B.W. Dijkstra, Model building of disulfide bonds in proteins with known three-dimensional structure, Protein Eng. 2 (1988) 119–125.

[19] W.F. van Gunsteren, H.J.C. Berendsen, Groningen Molecular Simulation (GROMOS) Library Manual, Biomos, Groningen, 1987.

[20] A.E. Mark, S.P. Helden, P.E. Smith, L.H.M. Janssen, W.F. van Gunsteren, Convergence properties of free energy calculations: α-cyclodextrin complexes as a case study, J. Am. Chem. Soc. 116 (1994) 6293–6302.

[21] L.W. Ungar, N.F. Scherer, G.A. Voth, Classical molecular dynamics simulation of the photo-induced electron transfer dynamics of plastocyanin, Biophys. J. 72 (1997) 5–17.

[22] R.M. Brunne, K.D. Berndt, P. Guntert, K. Wuthrich, W.F. van Gunsteren, Structure and internal dynamics of the bovine pancreatic trypsin inhibitor in aqueous solution from long-time molecular dynamics simulation, Proteins: Struct. Funct. Genet. 23 (1995) 49–62.

[23] A.E. Garcia, L. Stiller, Computation of the mean residence time of water in the hydration shells of biomolecules, J. Comp. Chem. 14 (1993) 1396–1406.

[24] P.H. Hünenberger, A.E. Mark, W.F. van Gunsteren, Fluctuation and cross-correlation analysis of protein motions observed in nanosecond molecular dynamics simulations, J. Mol. Biol. 252 (1995) 492–503.

[25] I. Ichiye, M. Karplus, Collective motions in proteins; a co-variance analysis of atomic fluctuations in molecular dynamics and normal modes simulations, Proteins: Struct. Funct. Genet. 11 (1991) 205–217.

[26] M.A. Balsera, W. Wriggers, Y. Oono, K. Schulten, Principal component analysis and long time protein dynamics, J. Phys. Chem. 100 (1996) 2567–2572.

[27] A.E. Garcia, G. Hummer, Conformational dynamics of cytochrome *c*: correlation to hydrogen exchange, Proteins: Struct. Funct. Genet. 36 (1999) 175–191.

[28] G. Vriend, WHAT IF — a molecular modeling and drug design program, J. Mol. Graph. 8 (1990) 52–56.

[29] E.I. Solomon, J.W. Hare, D.M. Dooley, J.A. Dawson, P.J. Stephens, H.B. Gray, Spectroscopic studies of stellacyanin, plastocyanin and azurin. Electronic structure of blue copper sites, J. Am. Chem. Soc. 102 (1980) 168.

[30] H.C. Freeman, Electron transfer in blue copper proteins, Coord. Chem. 21 (1981) 29–51.

[31] E. Fraga, M.A. Webb, G.R. Loppnow, Charge-transfer dynamics in plastocyanin, a blue copper protein from resonance Raman intensities, J. Phys. Chem. 100 (1996) 3278–3287.

[32] D.N. Beratan, J.N. Betts, J.N. Onuchic, Protein electron transfer rates set by the bridging secondary and tertiary structure, Science 252 (1991) 1285–1288.

[33] E.L. Gross, G.P. Andersson, S.L. Ketchner, J.E. Draheim, Plastocyanin conformation. The effect of nitrotyrosine modification and pH, Biochim. Biophys. Acta 808 (1985) 437–447.

[34] S.S. Skourtis, D.N. Beratan, High and low resolution theories of protein electron transfer, J. Biol. Inorg. Chem. 2 (1997) 378–386.

[35] H. Frauenfelder, F. Parak, R.D. Young, Conformational substates in proteins, Annu. Rev. Biophys. Biophys. Chem. 17 (1988) 451–479.

[36] R. Huber, W.S. Bennet, Functional significance of flexibility in proteins, Biopolymers 22 (1983) 261–279.

[37] G.M. Ullmann, E.-W. Knapp, N.M. Kostić, Computational simulation and analysis of dynamic association between plastocyanin and cytochrome *f*. Consequences for the electron-transfer reaction, J. Am. Chem. Soc. 119 (1997) 42–52.

[38] E.V. Pletneva, D.B. Fulton, T. Kohzuma, N.M. Kostić, Protein docking and gated electron-transfer reactions between zinc cytochrome *c* and the new plastocyanin from the Fern *Dryopteris crassirhizoma*. Direct kinetic evidence for multiple binary complexes, J. Am. Chem. Soc. 122 (2000) 1034–1046.

[39] K. Sigfridsson, S. Young, Ö. Hansson, Structural dynamics in the plastocyanin–photosystem 1 electron-transfer complex as revealed by mutant studies, Biochemistry 35 (1996) 1249–1257.

[40] D.M.F. van Aalten, A. Amadei, A.B.M. Linsenn, V.G.H. Eijsink, G. Vriend, H.J.C. Berendsen, The essential dynamics of thermolysin: confirmation of the hinge-bending motion and comparison of simulations in vacuum and water, Proteins: Struct. Funct. Genet. 22 (1995) 45–54.

[41] P.J. Kraulis, 'MOLSCRIPT': a program to produce both detailed and schematic plots of protein structures, J. Appl. Crystallogr. 24 (1991) 946–950.